

# AJNR

This information is current as  
of March 25, 2026.

## **Cone-Beam CT of the Temporal Bone: Normative Linear Biometry of Inner Ear Structures**

Giorgio Conte, Eliana Schifano, Elisa Massullo, Francesco  
Maria Lo Russo, Antonia Valentina Genovese, Silvia Casale,  
Elisa Scola, Federica Di Berardino, Lorenzo Maria Gaini,  
Diego Zanetti and Fabio Triulzi

*AJNR Am J Neuroradiol* published online 20 March 2026  
<http://www.ajnr.org/content/early/2026/03/19/ajnr.A9302>

# Cone-Beam CT of the Temporal Bone: Normative Linear Biometry of Inner Ear Structures

Giorgio Conte, Eliana Schifano, Elisa Massullo, Francesco Maria Lo Russo, Antonia Valentina Genovese, Silvia Casale, Elisa Scola, Federica Di Berardino, Lorenzo Maria Gaini, Diego Zanetti, and Fabio Triulzi

## ABSTRACT

**BACKGROUND AND PURPOSE:** Normative linear measurements of inner ear structures may enhance diagnostic accuracy in detecting subtle congenital abnormalities. This study aimed to establish Cone-Beam Computed Tomography (CBCT)-based normative reference values for temporal bone anatomy.

**MATERIALS AND METHODS:** We retrospectively reviewed consecutive CBCT scans of normal temporal bones acquired between June 2022 and June 2024. Scans were classified as normal based on the absence of pathological findings and no history of otologic disorders. Eleven linear measurements of inner ear structures were independently performed by two radiologists, and interobserver agreement was assessed. Reference centiles were generated for each parameter.

**RESULTS:** A total of 319 patients (135 men, 184 women; mean age, 50.03 years; range, 3 months–91 years) were included. Interobserver reliability was high across all measurements. Age and sex showed a small effect on any measurement. Normative centile distributions for all eleven structures were established.

**CONCLUSIONS:** This study provides robust CBCT-derived normative linear measurements of inner ear structures. These reference values may improve radiologic assessment of congenital hearing loss, particularly in patients with normal-appearing CT examinations.

**ABBREVIATIONS:** axCH = axial Cochlear Height; CBCT = Cone-Beam Computed Tomography; CNCW = Cochlear Nerve Canal Width; corCH = coronal Cochlear Height; CT = Computed Tomography; CW = Cochlear Width; IAC = Internal Auditory Canal; ICC = intraclass correlation coefficient; LSC = Lateral Semicircular Canal; LSCbi = bony island of the Lateral Semicircular Canal; MSCT = Multi-slices Computed Tomography; OW = Oval Window; RW = Round Window; SNHL = Sensorineural Hearing Loss; VAm = Vestibular Aqueduct at midpoint; VAO = Vestibular aqueduct at the external opening; VW = Vestibular Width

## INTRODUCTION

Computed tomography (CT) imaging is essential for evaluating the temporal bone, as it effectively visualizes the intricate and small bony structures of the inner ear. It serves as the primary diagnostic tool in cases of suspected otological disorders and is highly recommended in both preoperative and postoperative settings for providing critical anatomical information to surgeons and assessing surgical outcomes. Flat-Panel CT, or Cone-Beam computed tomography (CBCT), is increasingly recognized as the preferred imaging modality due to its superior image quality compared to multi-slice CT (MSCT). This is attributed to its

higher spatial resolution and isotropic voxel sizes as small as  $0.1 \text{ mm}^3$ . Although not yet widely available, CBCT offers the additional advantage of lower radiation exposure and reduces susceptibility to metallic artifacts,<sup>1,2</sup> which is particularly valuable for the post-surgical evaluation of cochlear implants and other prosthetic devices.

CT imaging is crucial for the diagnosis of inner ear malformations, which are found in 20% of patients with congenital sensorineural hearing loss (SNHL).<sup>3</sup> Although gross malformations (e.g. complete labyrinthine aplasia, cochlear aplasia or common cavity deformity) are easily detected on CT images, they represent only a small percentage of abnormal findings in patients with SNHL,<sup>4,5</sup> and subtle ear malformations can be often missed on CT evaluation. Normative linear measurement of inner ear structures could improve diagnostic sensitivity in detecting subtle ear malformations. In literature few studies have been conducted on healthy living subjects to assess normative biometry of the inner ear using MSCT<sup>6-9</sup> while no previous studies have been performed using CBCT.

The purpose of this study is to provide user-friendly normative linear references of inner ear structures using CBCT.

Received January 10, 2026; accepted after revision March 16.

From the Neuroradiology Unit (G.C., E.M., F.M.L.R., A.V.G., S.C., E.S., F.T.), Audiology Unit (F.D.B., D.Z.), Otolaryngology and Head and Neck Surgery (L.M.G.), Fondazione IRCCS Ca' Granda Ospedale Maggiore Policlinico, Milan, Italy; Department of Pathophysiology and Transplantation (G.C., F.T.), Clinical Sciences and Community Health (F.D.B., L.M.G., D.Z.), Università Degli Studi Di Milano, Milan, Italy; Diagnostic and Interventional Neuroradiology (E.S.), ARNAS Civico Di Cristina-Benfratelli, Palermo, Italy.

Corresponding Author: Elisa Massullo Neuroradiology Unit, Fondazione IRCCS Ca' Granda Ospedale Maggiore Policlinico Milan, Italy; e-mail: elisa.massullo@policlinico.mi.it

<http://dx.doi.org/10.3174/ajnr.A9302>

## SUMMARY

**PREVIOUS LITERATURE:** Inner ear malformations are present in about 20% of congenital sensorineural hearing loss cases, but subtle anomalies are frequently missed on qualitative CT assessment. Previous studies established normative linear measurements of inner ear structures using multi-slice CT (MSCT) in healthy subjects, reporting reference values for cochlear dimensions, vestibular aqueduct, semicircular canals, and windows. No prior publications have provided normative biometric data using Cone-Beam CT (CBCT), which offers superior spatial resolution (voxel size 0.14 mm) and reduced radiation dose compared to MSCT.

**KEY FINDINGS:** In 319 normal temporal bones examined with CBCT, 11 linear measurements showed high interobserver reliability (ICC). Distributions were non-normal; small age-related correlations and minor sex differences (small effect size) were observed in several parameters. Normative centiles (5–95%) were established for all structures.

**KNOWLEDGE ADVANCEMENT:** This is the first study to provide CBCT-specific normative reference values for inner ear linear measurements. These thresholds, derived from high-resolution imaging, enhance objective detection of subtle congenital malformations, support standardized reporting, improve diagnostic sensitivity in apparently normal scans, and facilitate comparison across different CT technologies.

## MATERIALS AND METHODS

### Study population

We retrospectively collected consecutive CBCT examinations of normal temporal bone which were performed at our institution between June 2022 and June 2024. Temporal bones were defined as normal according to the following criteria: 1) no pathologic findings on CBCT, and 2) no history of otologic disorders, evidenced by the patient's medical record. Each examination was performed to investigate or rule out suspected abnormalities in the contralateral temporal bone, including cholesteatoma, otosclerosis, inner and middle ear congenital malformations, and complications of otitis. The presence of common anatomical variants (e.g. high riding jugular bulb) or any alterations regarding the mastoid air cells and the external ear (e.g. external auditory canal exostoses, myringosclerosis or inflammatory opacification of the mastoid) were not considered as exclusion criteria. All procedures performed were in accordance with the ethical standards of the institutional and/or national research committee and with the 1964 Helsinki declaration and its later amendments or comparable ethical standards. Patient anonymity was guaranteed throughout the study. The reporting of this observational cohort study adheres to the STROBE guidelines (see Supplementary STROBE Checklist).

### CBCT acquisition and assessment

CBCT was performed with an angiographic system (Azurion, Philips Healthcare, Best, the Netherlands), including a digital flat panel detector, 30 × 40 cm with a source-to-image-receptor distance of 120 cm. Each temporal bone was scanned using the following scan parameters: current, 260 mA; voltage, 80 kV; FOV, 20 × 15 cm<sup>2</sup>; voxel size, 0.14 × 0.14 × 0.14 mm<sup>3</sup>; scan height, 150 mm. By rotating 240° (from 60° to 300°) passing through the posterior part of the head and avoiding the anterior part, the pivoting C-arm of the angiography unit acquires a volume dataset of up to 622 projections, with a scan time of 25 seconds. The dose-area product was 10,650 mGy × cm<sup>2</sup>, and the air kerma was 121 mGy. Postprocessing of this volume dataset was performed with reconstruction software (Allura 3D-RA 6.3.0/XperCt 3.1.0; Philips Healthcare).

### Inner and middle ear measurements

All CBCT examinations were reviewed by a senior neuroradiologist and a radiology resident with 12 years and 2 years of experience in otoradiology, respectively. Observers assessed measurements separately, with each measurement being taken twice (expressed in millimetres). The average of the two measurements was considered as the reference value and used for statistical analysis.

After a thorough review of the literature,<sup>4–10</sup> a total of 11 measurements of the bony structures of the inner ear were identified as reproducible and easy to apply during routine CT reporting. All measurements are summarized in Table 1 and Figures 1–2.

### Statistical analysis

The reliability of the measurements was evaluated using the intraclass correlation coefficient (ICC) with single fixed rates. Bland Altman plots were also drawn. We used the one-sample Kolmogorov-Smirnov test to investigate whether measurements were normal in distribution. Spearman's correlation test was adopted to evaluate the correlation of measurements with age, while the Wilcoxon test was used to test the relationship with sex. Statistical significance was set at p-value lower than 0.05. All statistical analyses were conducted using R Statistical Software (v4.4.2; R Core Team 2021).

## RESULTS

A total of 995 CBCT examinations were performed on 955 patients during the study period in our department. Thirty-eight patients underwent multiple CBCT examinations, only the first examination was considered for this study. Six-hundred and thirty-two patients were excluded due to bilateral temporal bone disease or because only the affected ear was scanned, four patients were excluded due to motion artifacts that affected the imaging quality. Finally, 319 CBCT examinations (130 right, 189 left) were analysed. Mean age of patients was 50.03 years (range: 3 months to 91 years), 135 (42.3%) patients were males and 184 (57.6%) females.

**Table 1: Description of measurements performed for each structure of the inner ear**

Ear structure	Description	Reference plane
Cochlear Nerve Canal Width (CNCW) [9] Fig.1A	The width of the bony canal for cochlear nerve at the entry of the cochlea is measured tangentially to the two inferior extremities of the X-shaped modiolus	Axial plane parallel to the LSC containing the modiolus in a clear "X" shape
Cochlear Width (CW) [9] Fig.1A	The maximum diameter of the cochlea is measured perpendicular to the cochlear nerve canal	
axial Cochlear Height (axCH) [9] Fig.1A	The height of the cochlea is defined as the length between the tip of the cochlea and the CNCW, parallel to the cochlear nerve canal	
Oval window (OW) Fig.1A	The maximum width of the oval window is measured	Coronal plane perpendicular to the oval window
coronal Cochlear Height (corCH) [6] Fig.1B	The maximal height is measured perpendicular to the oval window	
Vestibular aqueduct at midpoint (VAm) [7, 8] Fig.2A	The width of the vestibular aqueduct is measured perpendicular to both bony walls at the approximate midpoint determined by visually estimating the halfway point between the external aperture and the common crus	The Pöschl plane: a sagittal oblique reformat oriented perpendicularly to the longitudinal axis of petrous pyramid and parallel to the plane of the superior semicircular canal
Vestibular aqueduct at the external opening (VAo) [7] Fig.2A	The width of the vestibular aqueduct is measured perpendicular to both bony walls at the external opening in its largest dimension identified	
LSC bony island (LSCbi) [6] Fig.1C	The maximum diameter of the central bony island of the LSC	Axial plane parallel to the LSC
Vestibule width (VW) [6] Fig.1D	The maximum width is measured parallel to the long axis of the cochlear basal turn	
Internal auditory canal (IAC) Fig.2B	The width at the midpoint is measured perpendicular to the posterior wall of the IAC itself. The midpoint is defined between the fundus laterally and the line connecting the anterior and posterior border of the porus acusticus internus medially.	Axial plane oriented along the inferior wall of the IAC
Round window (RW) [10] Fig.2C	The width is measured in between the bony edges of the RW itself at the opening	Oblique plane parallel to the posterior semicircular canal

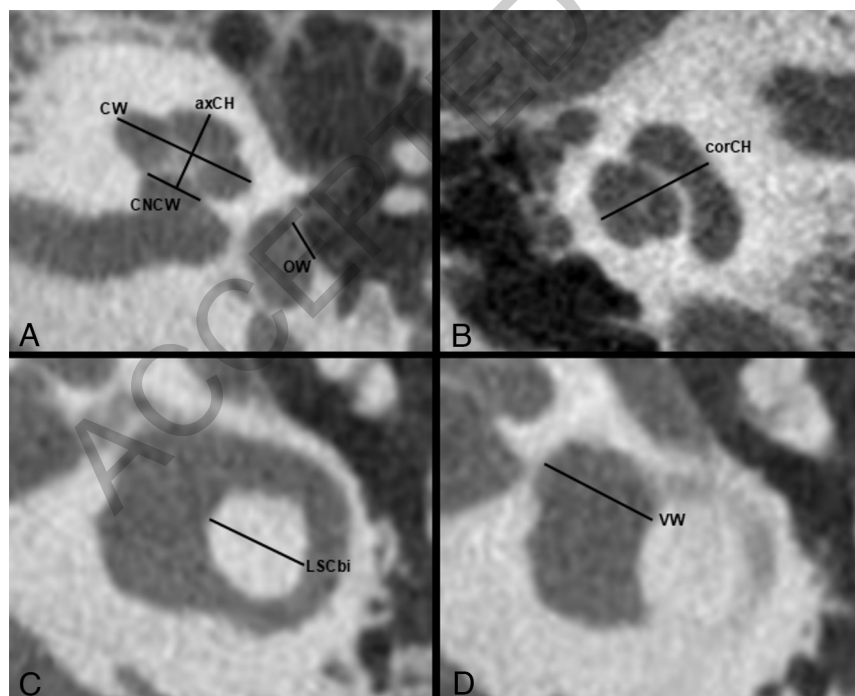


**FIG 1.** Measurement on the reference planes of (A) Cochlear Height on axial plane (axCH), Cochlear Nerve Canal Width (CNCW), Cochlear Width (CW), Oval Window (OW); (B) Cochlear Height on coronal plane (corCH); (C) LSC bony island (LSCbi); (D) Vestibule Width (VW).

Data about interobserver variability of the measurements are presented in Supplementary Table 1, with the corresponding Bland-Altman plots shown in Supplementary Figures 1-2. The measurements exhibited a non-normal distribution, as shown in Supplementary Table 2. Normative values and corresponding percentiles are reported in Table 2.

We found a very weak positive correlation with age for the cochlear nerve canal width (CNCW), for the cochlear width (CW), for both axial cochlear height (axCH) and coronal cochlear height (corCH), for the vestibule width (VW) and the oval window (OW). No other statistically significant correlations were observed between the remaining measurements and the age (Table 3; Supplementary Figures 3-4).

We observed sex differences in several measurements, including the CNCW, the CW, both axCH and corCH, the lateral semicircular canal bony island (LSCbi), the VW, as well as

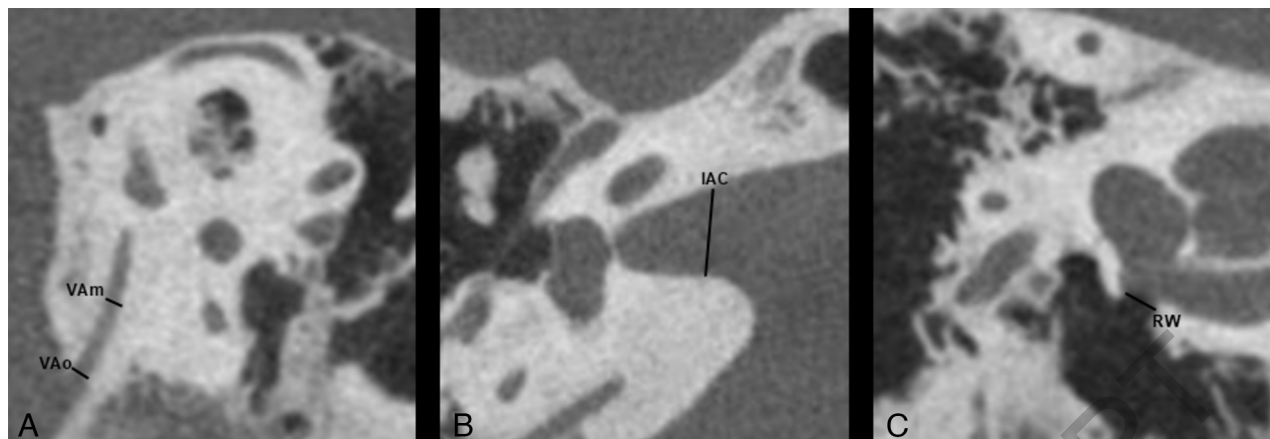


**FIG 2.** Measurements on the reference planes of (A) Vestibular Aqueduct at midpoint (VAm) and at the external opening (VAo); (B) Internal Auditory Canal (IAC); (C) Round Window (RW).

**Table 2: Reference centiles for each inner ear structure (mm)**

	5%	25%	50%	75%	95%
CNCW	1.8	2.0	2.2	2.3	2.6
CW	5.3	5.6	5.9	6.1	6.4
axCH	3.1	3.3	3.5	3.6	3.9
corCH	4.3	4.8	5.1	5.4	5.8
VAm	0.3	0.5	0.6	0.7	0.9
VAo	0.3	0.5	0.7	0.8	1.0
LSCbi	3.1	3.4	3.7	4.1	4.5
VW	2.8	3.2	3.4	3.6	3.9
IAC	3.1	3.7	4.2	4.8	6.0
RW	1.1	1.2	1.4	1.5	1.7
OW	2.0	2.2	2.3	2.5	2.8

axCH, axial cochlear height; CNCW, cochlear nerve canal width; corCH, coronal cochlear height; CW, cochlear width; IAC, internal auditory canal; LSCbi, bony island of the lateral semicircular canal; OW, oval window; RW, round window; VAm, vestibular aqueduct at midpoint; VAo, vestibular aqueduct at the external opening; VW, vestibular width.

**Table 3: Correlation of measurements with age evaluated with the Spearman's test**

	S	$\rho$	p-value
CNCW	4374473	0.1914457	< 0.001
CW	4660636	0.1385528	0.01
axCH	3953778	0.2692046	< 0.001
corCH	4811718	0.1106276	0.05
VAm	5548508	-0.02555663	0.6
VAo	4873969	0.09912155	0.08
LSCbi	5374133	0.006673803	0.9
VW	4695956	0.1320245	0.02
IAC	5493864	-0.01545666	0.8
RW	5515459	-0.01944808	0.7
OW	4526499	0.1633459	0.003

axCH, axial cochlear height; CNCW, cochlear nerve canal width; corCH, coronal cochlear height; CW, cochlear width; IAC, internal auditory canal; LSCbi, bony island of the lateral semicircular canal; OW, oval window; RW, round window; VAm, vestibular aqueduct at midpoint; VAo, vestibular aqueduct at the external opening; VW, vestibular width. Bold values indicate statistical significance.

both the OW and the round window (RW); all of which exhibit a small effect size (Table 4).

## DISCUSSION

This study provides 11 distinct normative measurements of inner ear structures that can be used for clinical CT imaging on a

**Table 4: Assessment of sex differences in measurements evaluated using the Wilcoxon test**

	W	p-value	effsize	magnitude
CNCW	9495	< 0.001	0.203	small
CW	9968.5	0.002	0.169	small
axCH	9940	0.002	0.172	small
corCH	10240	0.007	0.150	small
VAm	13058	0.4	0.0445	small
VAo	13070	0.4	0.0453	small
LSCbi	10379	0.01	0.141	small
VW	8841	< 0.001	0.247	small
IAC	11211	0.1	0.0832	small
RW	10770	0.04	0.115	small
OW	10687	0.03	0.120	small

axCH, axial cochlear height; CNCW, cochlear nerve canal width; corCH, coronal cochlear height; CW, cochlear width; effsize, effect size; IAC, internal auditory canal; LSCbi, bony island of the lateral semicircular canal; OW, oval window; RW, round window; VAm, vestibular aqueduct at midpoint; VAo, vestibular aqueduct at the external opening; VW, vestibular width. Bold values indicate statistical significance.

single-case basis. We found a minimal/absent effect of age and gender on these measurements and reference linear measurements were provided without distinguishing between age or sex. Our results align with the assumption that the bony labyrinth, as well as most other inner ear structures, does not change in size after birth.<sup>11</sup> A previous postmortem investigation including 27 paediatric subjects ranging from 12 hours to 12 years of age reported stable cochlear height and width across development.<sup>12</sup> A further large CT-based series of more than 400 ears demonstrated that cochlear height remains constant from infancy through adulthood, with only minor sex-related differences and no meaningful age-related growth.<sup>13</sup>

Few studies in the literature have addressed this topic. Nine (CNCW, CW, axCH, corCH, VAm, VAo, LSCbi, VW, RW) out of the 11 measurements were performed according to methodologies proposed in earlier studies,<sup>6-10</sup> and we found that the reference intervals were substantially overlapping,<sup>6-16</sup> confirming that normative values validated using MSCT are also applicable to CBCT, with the exception of the measurements related to the VW and RW. Reference values for the VW in the study by Shim et al.<sup>6</sup> were generally higher than ours, likely due to their axial resolution of 0.35 mm (versus 0.14 mm in our study), which may

have led to overestimation of actual dimensions, particularly in a morphologically variable structure such as the VW. The differences observed for the RW measurements, again higher than ours, may be attributed to the much smaller sample size in the study by Saylisoy et al,<sup>10</sup> in addition to the higher spatial resolution of our imaging technique.

We measured the internal auditory canal (IAC) using our own method, which appeared to be more easily applicable, and the results showed a very wide range, confirming the high variability of this structure, as also noted by other authors,<sup>5,6</sup> who do not consider it a clinically useful measurement. Only one study in the literature has assessed the width of the OW,<sup>17</sup> using a reference plane different from ours, making direct comparison not feasible. Considering the prevalence of subtle inner ear malformations, cochlear measurements (CW and corCH), VAm and VAo, and LSCbi appear to be the most clinically useful.

The establishment of standardized biometric reference values for inner ear structures offers a substantial contribution to radiologic assessment, particularly in the evaluation of congenital inner ear malformations. In complex malformative phenotypes, where multiple components of the labyrinth are affected, quantitative metrics provide an objective framework that supports systematic classification and reduces reliance on purely descriptive interpretation. Importantly, the value of biometric references extends to less complex or borderline malformations, in which morphologic abnormalities may be subtle, incomplete, or overlap with the spectrum of normal anatomic variability. In such cases, even expert radiologists may fail to recognize mild dimensional alterations or asymmetries on qualitative imaging assessment alone. The availability of normative biometric thresholds enables the identification of deviations that would otherwise remain unapparent, thereby improving diagnostic sensitivity and consistency. This quantitative approach is particularly relevant for surgical planning, including cochlear implantation, where unrecognized anatomic variations may have procedural or prognostic implications. Furthermore, biometric standardization enhances interobserver reproducibility and facilitates comparison across institutions and imaging platforms, strengthening both clinical decision-making and research applicability.

This study has several limitations that should be acknowledged. Although CBCT provides superior spatial resolution, our data essentially replicate established anatomic dimensions rather than providing new insights into inner ear anatomy or pathology. We recognize that these CBCT-derived normative values do not currently supplant existing MSCT-based references, but rather serve as an initial technical baseline for future, pathology-focused investigations. Its retrospective design restricted data collection to information available in-patient records, which may have resulted in incomplete or missing data. The study focused exclusively on linear measurements, which are easier to apply in clinical practice but may lack the sensitivity of volumetric assessments. Another limitation is that the study included only healthy ears, without a pathological comparison group. This limits the ability to determine whether the measured parameters can detect abnormalities in pathological conditions. Future studies should consider including a patient cohort, such as individuals

with SNHL, to further evaluate the applicability and sensitivity of these measurements. Nevertheless, despite the ears have been defined as healthy on the basis of clinical history and objective examination, the inclusion of patients with a contralateral otologic/audiological condition may represent a potential source of bias. Adjustments for multiple comparisons were not performed, which may increase the risk of type I error. Finally all examinations were performed using a single CBCT platform, which may limit the generalizability of our findings. While CBCT remains a clinically relevant imaging modality, emerging technologies such as photon-counting CT could potentially influence future normative standards, and should be considered in subsequent studies.

In conclusion, this study provides normative linear measurements of inner ear structures on CBCT that can enhance the imaging assessment of congenital deafness in clinical practice, particularly in cases where CT findings appear normal. Although CBCT provides superior spatial resolution, our data essentially replicate established anatomic CT-derived references. Further research including patient cohorts is warranted to validate diagnostic performance.

Disclosure forms provided by the authors are available with the full text and PDF of this article at [www.ajnr.org](http://www.ajnr.org).

## REFERENCES

1. Piergallini L, Scola E, Tuscano B, et al. **Flat-panel CT versus 128-slice CT in temporal bone imaging: Assessment of image quality and radiation dose.** *Eur J Radiol.* 2018;106:106–113 [CrossRef Medline](#)
2. Conte G, Scola E, Calloni S, et al. **Flat Panel Angiography in the Cross-Sectional Imaging of the Temporal Bone: Assessment of Image Quality and Radiation Dose Compared with a 64-Section Multisection CT Scanner.** *AJNR Am J Neuroradiol.* 2017;38(10):1998–2002 [CrossRef Medline](#)
3. Sennaroglu L. **Cochlear implantation in inner ear malformations—a review article.** *Cochlear Implants Int.* 2010;11(1):4–41 [CrossRef Medline](#)
4. D'Arco F, Talenti G, Lakshmanan R, Stephenson K, Siddiqui A, Carney O. **Do Measurements of Inner Ear Structures Help in the Diagnosis of Inner Ear Malformations? A Review of Literature.** *Otol Neurotol.* 2017;38(10):e384–e392 [CrossRef Medline](#)
5. Purcell D, Johnson J, Fischbein N, Lalwani AK. **Establishment of normative cochlear and vestibular measurements to aid in the diagnosis of inner ear malformations.** *Otolaryngol Head Neck Surg.* 2003;128(1):78–87 [CrossRef Medline](#)
6. Shim HJ, Shin JE, Chung JW, Lee KS. **Inner ear anomalies in cochlear implantees: importance of radiologic measurements in the classification.** *Otol Neurotol.* 2006;27(6):831–837 [CrossRef Medline](#)
7. Ozgen B, Cunnane ME, Caruso PA, Curtin HD. **Comparison of 45 degrees oblique reformats with axial reformats in CT evaluation of the vestibular aqueduct.** *AJNR Am J Neuroradiol.* 2008;29(1):30–34 [CrossRef Medline](#)
8. Juliano AF, Ting EY, Mingkwansook V, Hamberg LM, Curtin HD. **Vestibular Aqueduct Measurements in the 45° Oblique (Pöschl) Plane.** *AJNR Am J Neuroradiol.* 2016;37(7):1331–1337 [CrossRef Medline](#)
9. Teissier N, Van Den Abbeele T, Sebag G, Elmaleh-Berges M. **Computed Tomography measurements of the normal and the pathologic cochlea in children.** *Pediatr Radiol.* 2010;40(3):275–283 [CrossRef Medline](#)
10. Saylisoy S, Incesulu A, Kaya E, Pinarbasli O, Adapinar B. **The round window diameter in congenital aural atresia and comparison with sensorineural hearing loss and control group.** *J Comput Assist Tomogr.* 2014;38(3):461–463 [CrossRef Medline](#)

11. Som P.M, Curtin H.D, Liu K, and Mafee M.F. **Current Embryology of the Temporal Bone, Part I: the Inner Ear.** *Neurographics.* 2016; 6 (4):250–265 [CrossRef](#)
12. Eby TL, Nadol JB Jr. **Postnatal growth of the human temporal bone: implications for cochlear implants in children.** *Ann Otol Rhinol Laryngol* 1986;95(4 pt 1):356–64 [CrossRef Medline](#)
13. MC Mori and KW Chang. *American Journal of Neuroradiology.* 2012, 33 (1) 119–123 [CrossRef](#)
14. Purcell DD, Fischbein NJ, Patel A, Johnson J, Lalwani AK. **Two temporal bone computed tomography measurements increase recognition of malformations and predict sensorineural hearing loss.** *Laryngoscope.* 2006;116(8):1439–1446 [CrossRef Medline](#)
15. Chen JL, Gittleman A, Barnes PD, Chang KW. **Utility of temporal bone computed tomographic measurements in the evaluation of inner ear malformations.** *Arch Otolaryngol Head Neck Surg.* 2008;134(1):50–56 [CrossRef Medline](#)
16. Liu YK, Qi CL, Tang J, et al. **The diagnostic value of measurement of cochlear length and height in temporal bone CT multiplanar reconstruction of inner ear malformation.** *Acta Otolaryngol.* 2017;137(2):119–126 [CrossRef Medline](#)
17. Ukkola-Pons E, Ayache D, Pons Y, Ratajczak M, Nioche C, Williams M. **Oval window niche height: quantitative evaluation with CT before stapes surgery for otosclerosis.** *AJNR Am J Neuroradiol.* 2013;34(5):1082–1085 [CrossRef Medline](#)

ACCEPTED MANUSCRIPT

**Supplementary Table 1. Interobserver variability evaluation with intraclass correlation coefficient (ICC) with single fixed rates.**

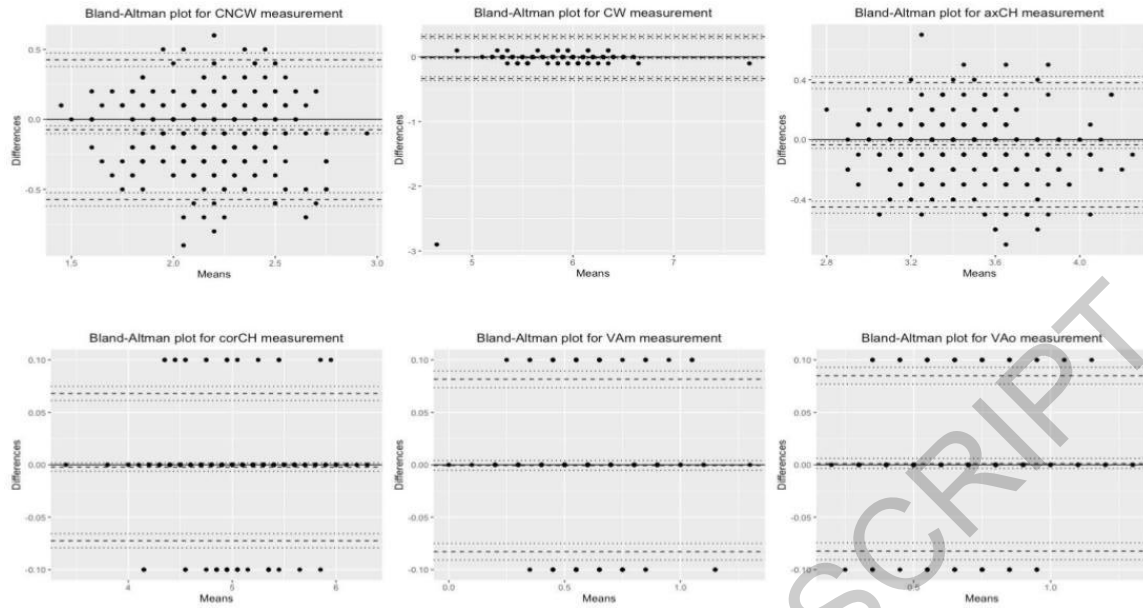
	ICC	p-value	lower bound	upper bound
CNCW	0.74	< 0.001	0.68	0.79
CW	0.89	< 0.001	0.87	0.91
axCH	0.84	< 0.001	0.80	0.87
corCH	1	0	1	1
VAm	0.98	< 0.001	0.97	0.98
VAo	0.98	< 0.001	0.98	0.98
LSCbi	1	0	1	1
VW	0.99	< 0.001	0.99	0.99
IAC	1	0	1	1
RW	0.98	< 0.001	0.98	0.99
OW	0.98	< 0.001	0.97	0.98

axCH, axial cochlear height; CNCW, cochlear nerve canal width; corCH, coronal cochlear height; CW, cochlear width; IAC, internal auditory canal; LSCbi, bony island of the lateral semicircular canal; OW, oval window; RW, round window; VAm, vestibular aqueduct at midpoint; VAo, vestibular aqueduct at the external opening; VW, vestibular width.

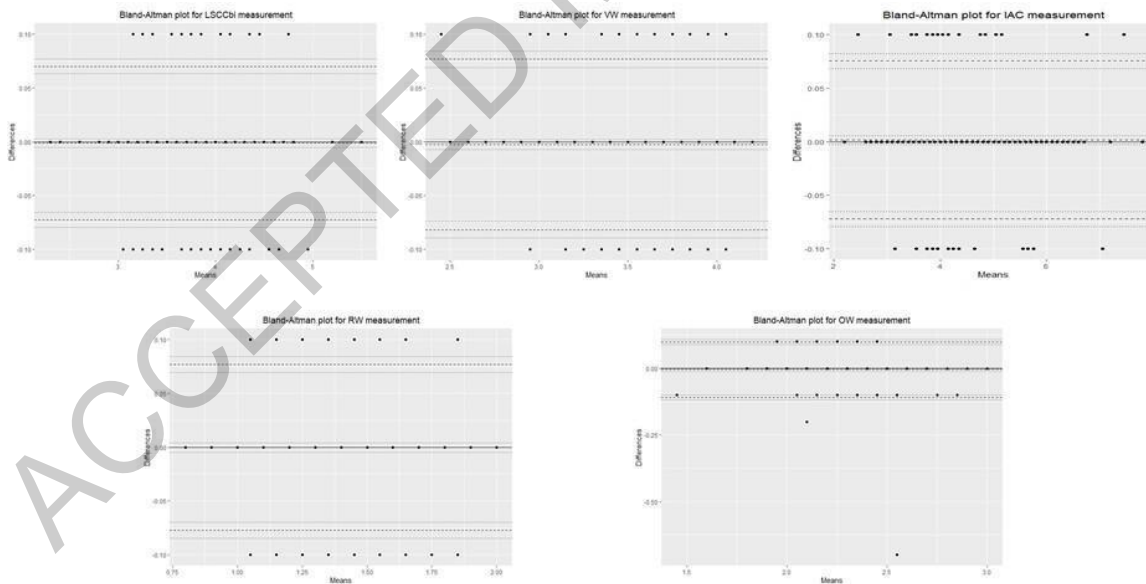
**Supplementary Table 2. Data distribution analysis using one-sample Kolmogorov-Smirnov test.**

	D	p-value
CNCW	0.93893	< 0.001
CW	0.9969	< 0.001
axCH	0.99744	< 0.001
corCH	0.99966	< 0.001
VAm	0.59005	< 0.001
VAo	0.61172	< 0.001
LSCbi	0.98618	< 0.001
VW	0.98871	< 0.001
IAC	0.98907	< 0.001
RW	0.82718	< 0.001
OW	0.95478	< 0.001

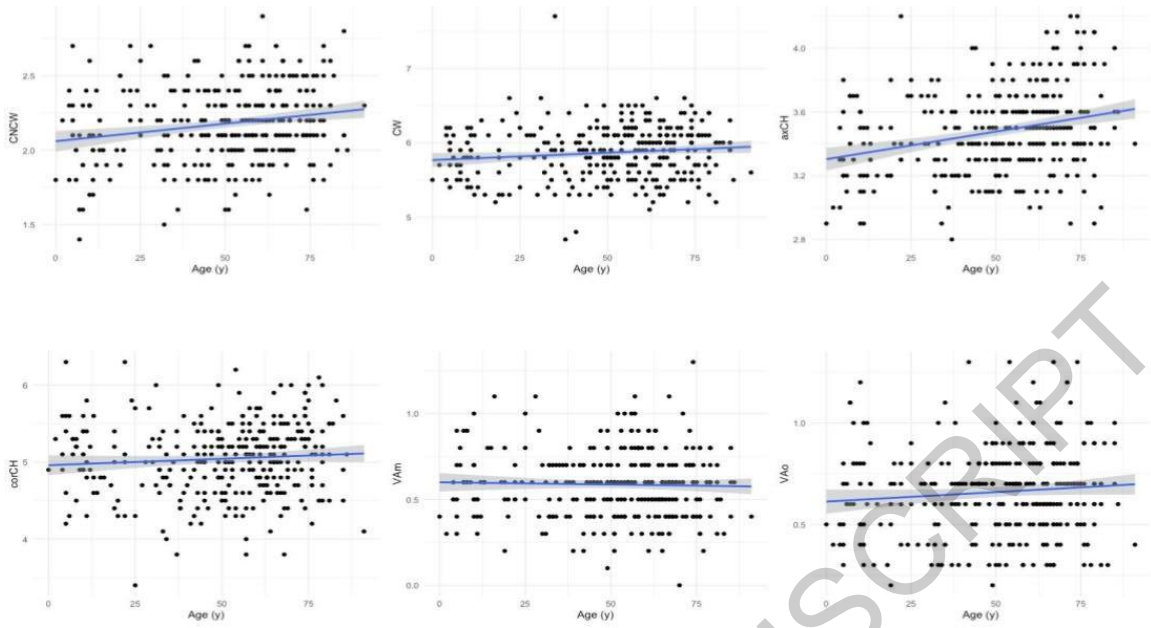
axCH, axial cochlear height; CNCW, cochlear nerve canal width; corCH, coronal cochlear height; CW, cochlear width; IAC, internal auditory canal; LSCbi, bony island of the lateral semicircular canal; OW, oval window; RW, round window; VAm, vestibular aqueduct at midpoint; VAo, vestibular aqueduct at the external opening; VW, vestibular width.



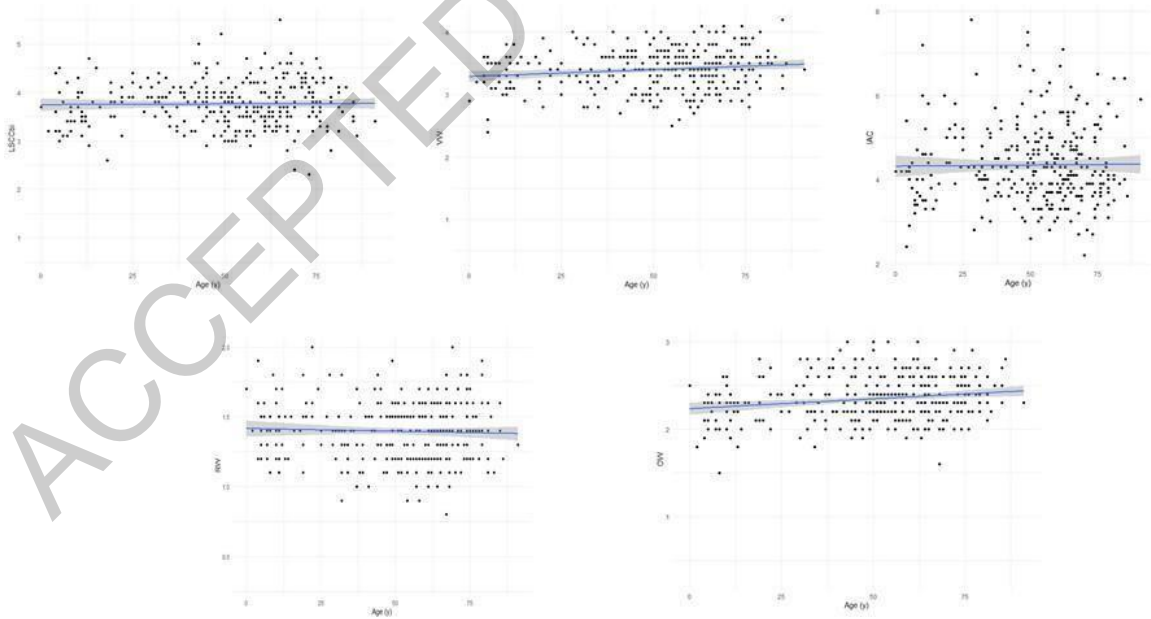
**Supplementary Figure 1.** Bland Altman plots for measurements of axCH, axial cochlear height; CNCW, cochlear nerve canal width; corCH, coronal cochlear height; CW, cochlear width; VAm, vestibular aqueduct at midpoint; VAo, vestibular aqueduct at the external opening.



**Supplementary Figure 2.** Bland Altman plots for measurements of IAC, internal auditory canal; LSCbi, bony island of the lateral semicircular canal; OW, oval window; RW, round window; VW, vestibular width.



**Supplementary Figure 3.** Scatter plot showing the relationship between age and data dispersion of axCH, axial cochlear height; CNCW, cochlear nerve canal width; corCH, coronal cochlear height; CW, cochlear width; VAm, vestibular aqueduct at midpoint; VAo, vestibular aqueduct at the external opening.



**Supplementary Figure 4.** Scatter plot showing the relationship between age and data dispersion of IAC, internal auditory canal; LSCbi, bony island of the lateral semicircular canal; OW, oval window; RW, round window; VW, vestibular width.